⌘ *Author's Choice*

THE JOURNAL OF BIOLOGICAL CHEMISTRY VOL. 286, NO. 19, pp. 17079–17090, May 13, 2011

Merkel Cell Polyomavirus Large T Antigen Disrupts Lysosome Clustering by Translocating Human Vam6p from the Cytoplasm to the Nucleus*

Received for publication, October 8, 2010, and in revised form, March 15, 2011 Published, JBC Papers in Press, March 16, 2011, DOI 10.1074/jbc.M110.192856

Xi Liu[‡], Jennifer Hein[‡], Simon C. W. Richardson[§], Per H. Basse[¶], Tuna Toptan[‡], Patrick S. Moore[‡1,2], Ole V. Gjoerup[‡1,3], and Yuan Chang[‡1,4]

From the [‡]Cancer Virology Program, [¶]University of Pittsburgh Cancer Institute, University of Pittsburgh, Pittsburgh, Pennsylvania 15213 and the [§]Department of Pharmaceutical, Chemical and Environmental Sciences, School of Science, University of Greenwich at Medway, Kent ME4 4TB, England

Merkel cell polyomavirus (MCV) has been recently described as the cause for most human Merkel cell carcinomas. MCV is similar to simian virus 40 (SV40) and encodes a nuclear large T (LT) oncoprotein that is usually mutated to eliminate viral replication among tumor-derived MCV. We identified the hVam6p cytoplasmic protein involved in lysosomal processing as a novel interactor with MCV LT but not SV40 LT. hVam6p binds through its clathrin heavy chain homology domain to a unique region of MCV LT adjacent to the retinoblastoma binding site. MCV LT translocates hVam6p to the nucleus, sequestering it from involvement in lysosomal trafficking. A naturally occurring, tumor-derived mutant LT (MCV350) lacking a nuclear localization signal binds hVam6p but fails to inhibit hVam6p-induced lysosomal clustering. MCV has evolved a novel mechanism to target hVam6p that may contribute to viral uncoating or egress through lysosomal processing during virus replication.

Merkel cell polyomavirus (MCV)[5] is a newly discovered human polyomavirus detected in ~80% of Merkel cell carcinomas (MCC) (1, 2). MCV encodes large T (LT), small T (ST), and 57kT transcripts similar to those of SV40 (2). These MCV T antigen sequences retain motifs found in other polyomavirus T antigens known to cause oncogenic transformation of rodent cells, such as an L*XCX*E (LFCDE) motif that binds to the retinoblastoma family of proteins and a DnaJ domain that interacts with heat-shock proteins (3–5). Significant mechanistic insights have been gained by identifying and characterizing cellular proteins that associate with polyomavirus T antigens. In addition to pRB and Hsc70, other cellular proteins linked to neoplastic transformation that interact with various T antigens include p53, Cul7, Bub1, PP2A, PI 3-kinase, and Shc (3, 4, 6–13). Identifying novel MCV T antigen binding partners is likely to provide critical insights into the mechanisms underlying MCV-induced tumorigenesis or viral replication.

MCV tumor-derived LTs have stop codon mutations that eliminate the helicase/ATPase domain but spare N-terminal L*XCX*E and DnaJ domains (2). Compared with SV40 T antigen, however, MCV T antigen contains a distinct 200-amino acid region, that we term the MCV T antigen unique region (MUR). MUR is located between the first exon and the origin-binding domain, and is conserved among tumor-derived MCV strains (14). Although MUR contains a partially conserved Bub1 binding motif similar that of SV40 LT (8), Bub1 does not appear to interact with MCV LT.[6] There are no other obvious features of MUR that might indicate its function for the virus.

We identified human Vam6p (hVam6p) by tandem-affinity pull-down of cellular proteins with a tagged MUR protein sequence. hVam6p is a cytoplasmic protein that promotes lysosome clustering and fusion *in vivo* through citron homology (CNH) and clathrin heavy chain repeat (CLH) domains (15). hVam6p also exhibits homology to the *Saccharomyces cerevisiae* vacuolar protein sorting 39 protein (Vps39). In yeast, membrane tethering is orchestrated at endosomes by the class C core vacuole/endosome transport (CORVET) complex and at lysosomes by the homotypic fusion and vacuole protein sorting (HOPS) complex. The HOPS complex is composed of the class C Vps complex (Vps11, Vps33, Vps18, Vps16) present in CORVET as well as Vps39 and Vps41 (16). Individual subunits appear to be conserved in mammalian cells. In addition to lysosomal metabolism, isoforms of hVam6p play roles in transforming growth factor-β (TGF-β) and mTOR signaling. hVam6p has been reported to be identical to an isoform of the TRAP-1-like protein that regulates the balance between Smad2 and Smad3 signaling through Smad4 interactions (17). Vam6/Vps39 in yeast has been shown to be a guanine nucleotide exchange factor for Gtr1, a Rag family GTPase that promotes

* This work was supported, in whole or in part, by National Institutes of Health Grants CA136363, CA120726 (to P. S. M. and Y. C.), and AI078926 (to O. V. G.) and University of Pittsburg Cancer Institute Core Facility Cancer Center Support Grant (CCSG) P30 CA047904, the Al Copeland Foundation for Merkel Cell Carcinoma Research, the University of Pittsburgh EXPLORER program, and American Cancer Society Research Professorships (to P. S. M. and Y. C.).

⌘ *Author's Choice*—Final version full access.

[1] These authors contributed equally to this work.

[2] To whom correspondence may be addressed. E-mail: psm9@pitt.edu.

[3] To whom correspondence may be addressed: 5117 Centre Ave., Suite 1.8, Pittsburgh, PA 15213. Tel.: 412-623-7721; Fax: 412-623-7715; E-mail: ovg27@pitt.edu.

[4] To whom correspondence may be addressed. E-mail: yc70@pitt.edu.

[5] The abbreviations used are: MCV, Merkel cell polyomavirus; MCC, Merkel cell carcinoma; LT, large T; ST, small T; MUR, MCV T antigen unique region; MBP, maltose-binding protein; TAP, tandem affinity purification; CNH, citron homology domain; CLH, clathrin homology domain; LAMP1, lysosomal-associated membrane protein 1; mTOR, mammalian target of rapamycin; TRITC, tetramethylrhodamine isothiocyanate; FITC, fluorescein isothiocyanate.

[6] O. Gjoerup, unpublished observations.

TORC1 activation in response to amino acid availability (18). In mammalian cells, hVam6p has been proposed to regulate mTORC1 signaling (19).

In this study we show that MCV LT binds hVam6p through a domain adjacent to the Rb-binding L*XCX*E motif and sequesters cytoplasmic hVam6p to the nucleus. This interaction is unique to MCV and does not occur with SV40 LT. Mislocalization of hVam6p by MCV LT inhibits hVam6p-induced lysosome clustering but does not have readily identifiable effects on TGF-β or mTOR signaling. This study shows that MCV modulates lysosomal clustering through a novel nuclear sequestration mechanism.

EXPERIMENTAL PROCEDURES

Plasmids—For generation of pNTAP-T4 and pNTAP-T5, the MCV sequence was amplified from the 5′ RACE product of MCV genomic LT (pcDNA3.1.MCV350) using primers MCV.861.BglII.S, 5′-GG AGA TCT AGT TGA CGA GGC CCC TAT ATA TGG G-3′; Exon2.1565.XhoI.AS, 5′-CG CTC GAG AGT AGG AAC AGG AGT TTC TCT G-3′; MCV.196.BglII.S, 5′-C GGG AGA TCT GGA TTT AGT CCT AAA TAG GAA AGA AAG-3′; Exon2.1565.XhoI.AS, 5′-CG CTC GAG AGT AGG AAC AGG AGT TTC TCT G-3′. The BglII/XhoI-digested fragments were cloned into pNTAP-B (Stratagene) using BamHI and XhoI restriction sites. pcDNA3.1.MCV350 was generated using MCC350 tissue DNA as template and primers 350.FLT.KpnI.F2.S, 5′-GG GGT ACC CAG CTC ATT TGC TCC TCT GCT G TT TCT-3′ and 350.FLT.XhoI.R, 5′-CCG CTC GAG CGG TGG GTC TAT TCA GAC AGG CTC T-3′. The PCR product was digested with KpnI/XhoI and cloned into pcDNA3.1/Zeo vector (Invitrogen). To generate pNTAP-SV40.T1–136, pCMV.SV40.LT was amplified using primers T1–136.S, 5′-CCT TTA GGA TCC GCC ATG GAT AAA GTT TTA AAC AGA-3′, and T1–136.AS, 5′-CCT TTA GGA TCC TTA CTT GGG GTC TTC TAC C-3′. The PCR product was digested with BamHI and cloned into pNTAP-B (Stratagene). Construction of gLT-V5, LT-V5, cLT339-V5, and cLT350-V5 expression plasmids were described previously (2). LT-EGFP, cLT339-EGFP, and cLT350-EGFP were constructed using inserts from LT-V5, cLT339-V5, and cLT350-V5 digested with NheI/SacII and cloned into pEGFP-N1 (Clontech). SV40.LT-EGFP was amplified from pCMV.SV40.LT and cloned into pEGFP-N1 (Clontech).

To generate GST fusion MCV LT truncations GST-LT(1–258), GST-LT(79–170), GST-LT(171–258), GST-LT(171–218), and GST-LT(219–258), pcDNA6.LT-V5 (2) were amplified using primers: pGEX.LT.1–78.BglII(S), 5′-CCT TTA AGA TCT GCC ATG GAT TTA GTC CTA AAT AGG-3′ and pGEX.LT.1–258.BglII(AS), 5′-CCT TTA AGA TCT TTA ATC TGT AAA CTG AGA TGA CG-3′; pGEX.LT.79–258.BglII.S, 5′-CCT TTA AGA TCT GCC GTT GAC GAG GCC CCT ATA TAT GGG-3′; pGEX.LT.79–170.BglII.AS, 5′-CCT TTA AGA TCT TTA TTC CTC ATG GTG TTC GGG AGG-3′; pGEX.LT.171–258.BglII.S, 5′-CCT TTA AGA TCT GCC CCC ACC TCA TCC TCT GGA TCC-3′; pGEX.LT.1–258.BglII.AS, 5′-CCT TTA AGA TCT TTA ATC TGT AAA CTG AGA TGA CG-3′; pGEX.LT.171–258.BglII.S, 5′-CCT TTA AGA TCT GCC CCC ACC TCA TCC TCT GGA TCC-3′; pGEX.LT.171–218.BglII.AS, 5′-CCT TTA AGA TCT TTA AAG TGA TTC ATC GCA GAA GAG-3′; pGEX.LT.219–258.BamHI.S, 5′-CCT TTA GGA TCC GCC TCC TCC CCT GAG CCT CCC TCG-3′; pGEX.LT.1–258.BglII.AS, 5′-CCT TTA AGA TCT TTA ATC TGT AAA CTG AGA TGA CG-3′. The BglII digested 1–258, 79–170, 171–258, and 171–218, and BglII/BamHI digested 219–258 fragments were cloned into pGEX4T-2 using a BamHI restriction site. For the GST fusion LT deletion mutant, GST.dl171–181, GST.dl182–192, GST.dl193–203, and GST.dl204–218 were generated by the QuikChange Lighting Site-directed Mutagenesis Kit (Agilent) using GST.LT(1–258) as a template and the following primer pairs: dl171–181.S, 5′-CCT CCC GAA CAC CAT GAG GAA GAG ACC ACC AAT TCA GGA AGA-3′ and dl171–181.AS, 5′-TCT TCC TGA ATT GGT GGT CTC TTC CTC ATG GTG TTC GGG AGG-3′; dl182–192.S, 5′-CCT CTG GAT CCA GTA GCA GAG AGC CCA ATG GAA CCA GTG TAC CTA G-3′ and dl182–192.AS, 5′-CTA GGT ACA CTG GTT CCA TTG GGC TCT CTG CTA CTG GAT CCA GAG G-3′; dl193–203.S, 5′-CAG GAA GAG AAT CCA GCA CAA GAA CGT ATG GCA CCT GGG A-3′ and dl193–203.AS, 5′-TCC CAG GTG CCA TAC GTT CTT GTG CTG GAT TCT CTT CCT G-3′; dl204–218.S, 5′-CCA GTG TAC CTA GAA ATT CTT CCT CCT CCC CTG AGC CTC CCT CGT C-3′ and dl204–218.AS, 5′-GAC GAG GGA GGC TCA GGG GAG GAG GAA GAA TTT CTA GGT ACA CTG G-3′.

MCV LT alanine substitution mutants, GST.LT(1–258).R204A, T205A, Y206A, G207A, T208A, and W209A were generated using the QuikChange Lighting Site-directed Mutagenesis Kit (Agilent) using GST.LT(1–258) as a template and the following primer pairs: R204A.S, 5′-CCT AGA AAT TCT TCC GCA ACG GAT GGC ACC TGG-3′ and R204A.AS, 5′-CCA GGT GCC ATC CGT TGC GGA AGA ATT TCT AGG-3′; T205A.S, 5′-GAA ATT CTT CCA GAG CGG ATG GCA CCT GGG-3′ and T205A.AS, 5′-CCC AGG TGC CAT CCG CTC TGG AAG AAT TTC-3′; Y206A.S, 5′-GAA ATT CTT CCA GAA CGG CTG GCA CCT GGG AGG ATC-3′ and Y206A.AS, 5′-GAT CCT CCC AGG TGC CAG CCG TTC TGG AAG AAT TTC-3′; G207A.S, 5′-CTT CCA GAA CGG ATG CCA CCT GGG AGG ATC TC-3′ and G207A.AS, 5′-GAG ATC CTC CCA GGT GGC ATC CGT TCT GGA AG-3′; T208A.S, 5′-CCA GAA CGG ATG GCG CCT GGG AGG ATC TCT TC-3′ and T208A.AS, 5′-GAA GAG ATC CTC CCA GGC GCC ATC CGT TCT GG-3′; W209A.S, 5′-GAA CGG ATG GCA CCG CGG AGG ATC TCT TCT GC-3′ and W209A.AS, 5′-GCA GAA GAG ATC CTC CGC GGT GCC ATC CGT TC-3′. The LT.W209A-V5 mutant was made by site-directed mutagenesis of pcDNA6.LT-V5 (2) using PCR primers: W209A.S, 5′-GAA CGG ATG GCA CCG CGG AGG ATC TCT TCT GC-3′ and W209A.AS, 5′-GCA GAA GAG ATC CTC CGC GGT GCC ATC CGT TC-3′. The Rb binding domain mutant, gLT.LXCXK-V5 was described previously (2).

To generate pDsRed.LT, LT-GFP was used as template using primers: pDsRed.LT.XhoI.S, 5′-CCG CTC GAG ATG GAT TTA GTC CTA AAT AGG-3′ and pDsRed.LT.XmaI.AS, 5′-CCC CCC GGG GTT GAG AAA AAG TAC CAG AAT

C-3′. The XhoI/XmaI-digested fragments were cloned into pDsRed-Monomer-Hyg-N1 (Clontech) using XhoI and XmaI restriction sites. pDsRed.LT.W209A was made by site-directed mutagenesis of pDsRed.LT using PCR primers: W209A.S, 5′-GAA CGG ATG GCA CCG CGG AGG ATC TCT TCT GC-3′ and W209A.AS, 5′-GCA GAA GAG ATC CTC CGC GGT GCC ATC CGT TC-3′.

To generate GST fusions of full-length LT (GST-LT) and LT hVam6p binding mutant (GST-LT.W209A), pcDNA6.LT-V5 (2) and pcDNA6.LT.W209A-V5 (described above) were digested with EcoRV and XhoI. These fragments were cloned into pALEX vector, which was first digested with NotI, subsequently treated with mung bean exonuclease, and further digested with XhoI. To generate maltose-binding protein-tagged hVam6p (MBP-hVam6p), hVam6p was amplified using 5′-CG GGA TCC CAC GAC GCT TTC GAG CC-3′ and 5′-GC TCT AGA TCA AGT GTC AGC TGG GTT TAC-3′ primer pairs. The BamHI- and XbaI-digested PCR product was then inserted into the corresponding restriction sites of the pMAL-2c vector (New England BioLabs).

pXS-HA-hVam6p and pXS-Myc-hVam6p were kindly provided by Dr. Juan S. Bonifacino (15). mVps39.FL-GFP, mVps39.Nter-GFP, mVps39.Cter-GFP, and mVps39.CNH-GFP constructs were kindly provided by Dr. J. Paul Luzio (20). To generate mVps39.Δ(CNH+CLH)-GFP, mVps39.FL-GFP was used as template using primers: pEGFP.mVps39.dl.KpnI.S, 5′-CGG GGT ACC GTG CTG AGA GAC TTC-3′ and pEGFP.mVps39.dl.BamHI.AS, 5′-CGC GGA TCC TCA GGT GTC GGC TGA-3′. The KpnI/BamHI-digested fragment was cloned into pEGFP-C1 (Clontech).

Cell Culture and Transfection—U2OS (ATCC), 293 (ATCC), 293H (Invitrogen), 293FT (Invitrogen), HT1080 (ATCC), and HeLa (ATCC) cells were maintained in DMEM (Mediatech) supplemented with 10% fetal bovine serum (FBS) at 37 °C in a 5% CO_2 incubator. Cells in 100-mm or 12-well plates (60% confluence) were transfected 24 h after plating with 6 or 2 μg of plasmid DNA using FuGENE-6 (Roche Applied Science) following the manufacturer's instructions. UISO (2), MCC13 (2), MCC26 (2), MKL-1 (2), MS-1 (21), and WaGa (21) were grown in RPMI 1640 (Sigma) supplemented with 10% FBS.

Tandem Affinity Purification (TAP)—293H cells transfected with pNTAP.SV40.T1–136, pNTAP.MCV.T4, and pNTAP.MCV.T5 were resuspended in lysis buffer containing protease inhibitor mixture (Roche Applied Science) and 0.1 mM PMSF. Cells were subjected to three successive rounds of freeze-thaw by incubating on dry ice for 10 min then in cold water for 10 min. Supernatant was collected after centrifugation at 16,000 × *g* for 10 min. 0.5 M EDTA and 14.4 M β-mercaptoethanol (Stratagene InterPlay Mammalian TAP System) were added. Washed streptavidin resin (50% slurry) was added to the lysate, followed by rotation at 4 °C for 2 h to allow tagged proteins to bind. Resin was collected by centrifugation at 1,500 × *g* for 5 min and washed twice in 1 ml of streptavidin binding buffer. Streptavidin elution buffer was added to the resin, followed by rotation at 4 °C for 30 min to elute protein complexes. The resin was centrifuged at 1,500 × *g* for 5 min and the supernatant was transferred to a fresh tube. Streptavidin supernatant supplement, calmodulin binding buffer, and the washed calmodulin resin (50% slurry) were added to the supernatant, followed by rotation at 4 °C for 2 h to allow protein complexes to bind to the calmodulin resin. Then the resin was washed twice in calmodulin binding buffer and collected by centrifugation at 1,500 × *g* for 5 min. Calmodulin elution buffer was added to the calmodulin resin and rotated at 4 °C for 30 min to elute protein complexes. Supernatant containing purified protein complexes was collected after centrifugation.

Mass Spectrometric Analysis—Individual protein bands were excised from polyacrylamide gels and washed twice with 50% acetonitrile in HPLC grade water and sent to the Mass Spectrometry Core Facility at Beth Israel Deaconess Medical Center, Boston, MA, for characterization.

Antibodies—Anti-MCV LT antibody CM2B4 was generated as previously described (22). hVam6p rabbit polyclonal antibody was kindly provided by Dr. Robert C. Piper (23). Anti-V5 rabbit antibody (Bethyl Laboratories), anti-HA.11 clone 16B12 monoclonal antibody (Covance), rabbit polyclonal recognizing GFP (Abcam), anti-Myc tag clone 4A6 antibody (Millipore), purified mouse anti-human retinoblastoma protein antibody (BD Pharmingen), anti-human CD107a (LAMP1) Alexa Fluor 488 (eBioscience), phospho-4EBP-1 Thr-37/46 (Cell Signaling), phospho-4EBP-1 Ser-65 (Cell Signaling), anti-mouse secondary antibody (GE Healthcare), and anti-rabbit secondary antibody (Sigma) were purchased commercially. hVam6p/Vps39 antibodies tested include rabbit polyclonal catalog number 16219-1-AP (Proteintech), goat polyclonals sc-104759 and sc-104761 (Santa Cruz), mouse polyclonal ab69669 (Abcam), and rabbit polyclonal ab90516 (Abcam).

Immunoprecipitation—U2OS cells were co-transfected with pXS-HA-hVam6p and either pcDNA6/V5-HisB plasmid (Invitrogen) or LT plasmid (pcDNA6.gLT-V5, cLT-V5, cLT339-V5, cLT350-V5) using FuGENE-6 (Invitrogen). Cells were harvested 48 h after transfection suspended in lysis buffer (50 mM Tris-HCl, 0.15 M NaCl, 1.5% Nonidet P-40, pH 7.4) supplemented with protease inhibitors. Precleared lysates were immunoprecipitated with rabbit anti-V5 (Bethyl) for 2 h at 4 °C. Lysates were incubated with Protein A/G-Sepharose beads (Santa Cruz) for 1 h at 4 °C, collected, and washed with lysis buffer. Beads were resuspended in 3 × SDS loading buffer and proteins were separated by SDS-PAGE. Immunoblotting was performed with anti-HA (Covance).

Immunoblot Analysis—Transfected cells were lysed in buffer (40 mM Tris-HCl, pH 7.4, 120 mM NaCl, 0.5% Triton, 0.3% SDS) containing protease inhibitor mixture (Roche Applied Science). Sonicated lysates were electrophoresed in 10% SDS-PAGE, transferred to nitrocellulose membrane (GE Healthcare), and reacted with anti-HA (1:1,000 dilution, Covance) overnight at 4 °C, followed by anti-mouse IgG-HRP conjugates (1:3,000 dilution, GE Healthcare) for 1 h at room temperature. Detection of peroxidase activity was performed by Western Lightning Plus-ECL reagent (PerkinElmer Life Sciences).

Immunofluorescence Analyses—For high resolution microscopy, cells were fixed with 4% paraformaldehyde for 20 min, permeablized with phosphate-buffered saline (PBS) with 0.2% Triton X-100, blocked with 10% BSA, and then incubated with anti-Myc (1:100 dilution, Millipore) overnight at 4 °C. Secondary antibody (Alexa Fluor 568-conjugated anti-mouse or Alexa

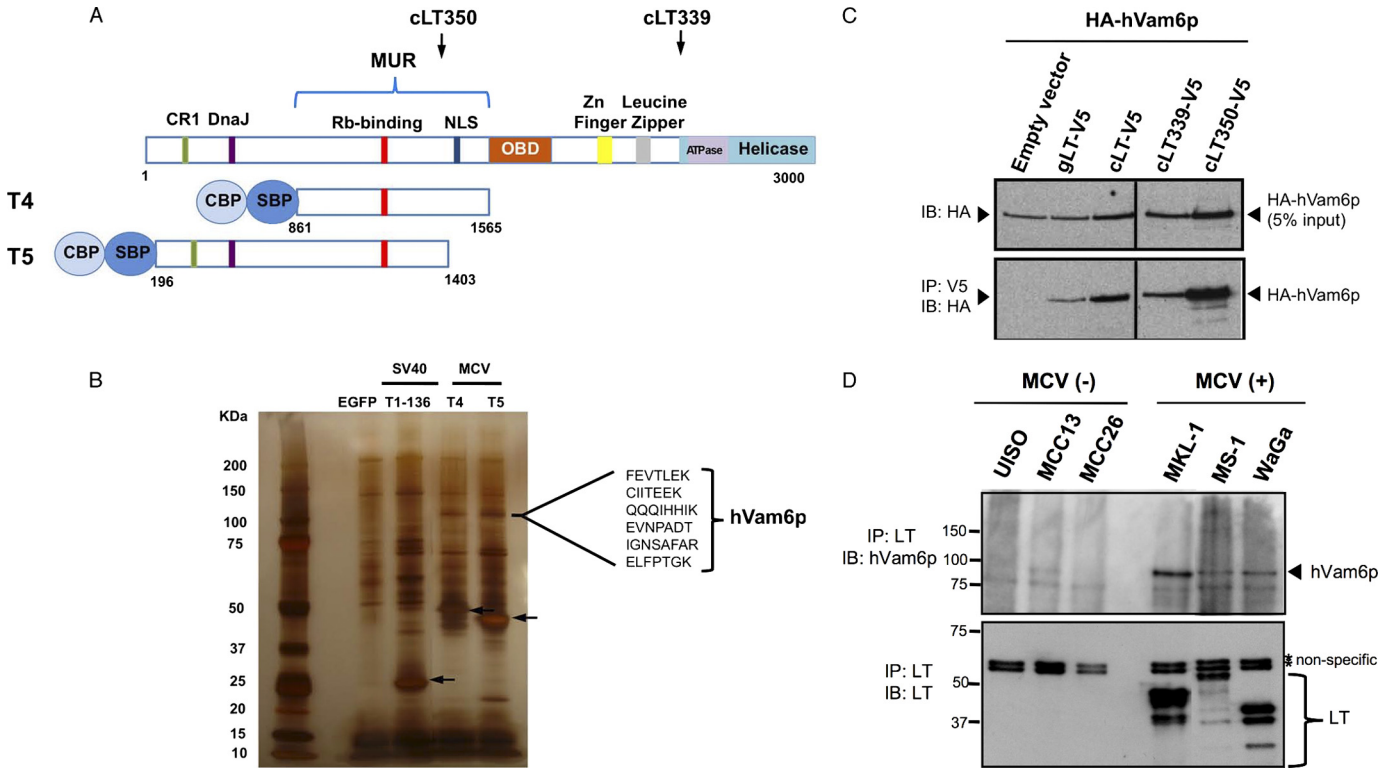

FIGURE 1. **Identification of hVam6p as an MCV LT interactor.** *A*, schematic diagram of MCV LT showing the site of the MUR and location of T4 and T5 LTs fused to N-terminal dual tags and used for TAP experiments. Positions of tumor-derived T antigen truncations cLT350 and cLT339 are shown (*arrows*). NLS, nuclear localization signal (30); *CBP*, calmodulin-binding protein; *SBP*, streptavidin-binding protein. *B*, silver stain of SDS-PAGE gel separating protein lysates after TAP isolation. *Arrows* indicate various TAP-tagged LT proteins stably expressed in 293H cell lines. A 120-kDa band, present only in MCV LT TAP from T4 and T5, was excised for mass spectrometric analysis. hVam6p peptide sequences identified from these bands are shown. *C*, lysates from U2OS cells transiently overexpressing HA-hVam6p and V5-tagged LTs were immunoprecipitated for LT with anti-V5 antibody and immunoblotted for hVam6p using anti-HA antibody. *D*, endogenous LT-hVam6p interaction in MCV-negative and MCV-positive cell lines. MCV LT is detected only in MCV-positive cell lines (MKL-1, MS-1, and WaGa) and LT immunoprecipitation pulls down endogenous hVam6p protein.

Fluor 488-conjugated anti-mouse, 1:1,000 dilution, Invitrogen) was incubated for 1 h at room temperature. All antisera were diluted in 1% BSA in PBS, and intervening washes of slides were carried out three times with PBS for 15 min. For the LAMP1 clustering experiment, transfected HeLa cells were fixed and permeabilized in PBS with 10% FCS, 2% paraformaldehyde, 0.3% saponin for 15 min at room temperature as previously described (24). Cells were washed twice in PBS with 0.03% saponin before and after staining with anti-human CD107a (LAMP1) Alexa Fluor 488 (eBioscience). Cells were counterstained with 4′,6′-diamidino-2-phenylindole (DAPI) and examined under a fluorescence microscope (AX70, Olympus).

Confocal Microscopy—MKL-1 cells were fixed with 4% paraformaldehyde for 20 min at 4 °C, permeablized with PBS with 0.2% Triton X-100, blocked with 10% BSA, incubated with rabbit polyclonal anti-hVam6p (1:100 dilution, from Dr. Robert C. Piper (23)) for 4 h at room temperature, followed by incubation with mouse anti-Lamin B1 (1:50 dilution, ZYMED) overnight at 4 °C. Secondary antibody (Alexa Fluor 488-conjugated anti-mouse and Alexa Fluor 568-conjugated anti-rabbit, 1:1,000 dilution, Invitrogen) was applied for 1 h at room temperature. Cells were stained with DRAQ5 (1:1,000 in PBS, Biostatus) for 10 min at room temperature, washed in PBS for 10 min, and mounted with VECTASHIELD mounting medium for fluorescence (Vector Laboratories, Inc.). Confocal images were acquired using a Leica TCSSL confocal microscope.

Glutathione S-Transferase (GST) Fusion Purification and GST Pull-down Assay—Cultures of JM109 bacterial host cells expressing GST fusion plasmids were grown overnight, followed by subculture (1:10) into 250 ml of LB with ampicillin. After 1 h, isopropyl β-D-1-thiogalactopyranoside was added at 0.5 mM final concentration. Induced cultures were grown for another 3–4 h and harvested by centrifugation at 3,000 × *g* for 10 min. Cell pellets were resuspended in cold NETN (0.5% Nonidet P-40, 1 mM EDTA, 50 mM Tris, pH 8.0, 120 mM NaCl) containing protease inhibitors, followed by sonication. Supernatants were collected by centrifugation and 300 μl of glutathione-Sepharose 4B beads (GSH beads, 50% slurry in NETN) were added followed by incubation at 4 °C for 30 min. GSH beads were washed 5 times with NETN buffer. For the binding assay, 293FT cells were transiently transfected with HA-hVam6p and harvested 48 h after transfection in NETN lysis buffer in the presence of protease inhibitors. Lysates were precleared using 20 μl of GSH beads loaded with GST (pGEX4T-2) for 1 h at 4 °C. Complexes were collected by addition of 30 μl of GSH beads loaded with appropriate fusion protein, rotation was for 2 h at 4 °C followed by centrifugation. The isolated beads were washed three times for 30 min at 4 °C with NETN and eluted with 50 μl of freshly made elution buffer (25 mM glutathione, 50 mM Tris-HCl, pH 8.8, 200 mM NaCl, pH 8.8). Elution samples were resuspended in 3× SDS loading buffer

and proteins were separated by SDS-PAGE using 10% polyacrylamide gels. Immunoblotting was performed with anti-HA (Covance).

MBP Fusion Purification and MBP Pull-down Assay—GST-LT, GST-LT.W209A, and MBP-hVam6p were expressed in *Escherichia coli* Rosetta (DE3) pLysS and BLR(DE3) (Novagen), respectively, and induced with 0.5 mM isopropyl β-D-1-thiogalactopyranoside for 2 h at 37 °C. Cells were harvested by centrifugation at 6,000 × *g* for 15 min at 4 °C. GST fusion proteins were extracted in lysis buffer (0.5% Nonidet P-40, 250 mM NaCl, 50 mM Hepes/KOH, pH 7.6, 1 mM EDTA, pH 7.4) supplemented with 0.2 mg/ml of lysozyme and protease inhibitor mixture (Roche Applied Science). MBP-hVam6p was extracted in ice-cold column buffer (200 mM NaCl, 20 mM Tris-HCl, pH 7.4, 1 mM EDTA, 0.02% NaN_3) supplemented with 0.2 mg/ml of lysozyme, 1 mM DTT, and 1 mM PMSF. The suspensions were incubated for 20 min on ice. Following repeated freeze-thaw cycles, cells were sonicated on ice and centrifuged at 10,000 × *g* for 30 min at 4 °C. For purification of fusion proteins, cleared supernatants were incubated with 1/100th volume of equilibrated glutathione-Sepharose 4B beads (GE Healthcare) or amylose resin (New England Biolabs) for 30 min at room temperature or 2 h at 4 °C, respectively. Beads were collected by centrifugation at 1,000 × *g* for 1 min and washed four times with lysis buffer. Fusion proteins were eluted by addition of 10 mM reduced glutathione, 50 mM Tris-HCl, pH 8.0, or 30 mM maltose, 50 mM Tris-HCl, pH 8.0, followed by silver staining analysis.

For the pull-down experiment, MBP-hVam6p-bound amylose resin beads were incubated with eluted GST, GST-LT, or GST-LT.W209A proteins for 2 h at 4 °C in binding buffer (0.5% Nonidet P-40, 120 mM NaCl, 50 mM Tris, pH 8.0, and 1 mM EDTA) supplemented with protease inhibitor mixture (Roche Applied Science). Beads were washed three times with binding buffer for 30 min at 4 °C, resuspended in SDS loading buffer, boiled for 10 min, and proteins were separated on a 8% SDS-PAGE gel. Immunoblotting was performed with anti-MCV LT antibody CM2B4 (22) and anti-MBP (New England Biolabs).

TGF-β-inducible Luciferase Reporter Assays—HT1080 cells were transfected with the TGF-β-inducible reporter p3TP-Lux (Addgene) and empty vector, wild-type LT, hVam6p binding mutant LT, alone or together with hVam6p. The p3TP-Lux reporter contains three 12-*O*-tetradecanoylphorbol 13-acetate response elements from the human collagenase promoter and the TGF-β responsive element from the plasminogen activator inhibitor-1 promoter ligated upstream to the adenovirus E4 minimal promoter (25). 24 h after transfection, cells were replaced with fresh DMEM with 0.2% FBS, left non-treated or treated with recombinant human TGF-β1 (Invitrogen) at 5 ng/ml for 18 h. Transfection efficiency was normalized with pRL-null vector (Promega). *Renilla* and *firefly* luminescence activities were measured using the Dual Luciferase Reporter Assay System (Promega) on a microplate luminescence counter (TopCount-NXT™, Packard).

RESULTS

MCV Large T Antigen Associates with hVam6p—To identify novel cellular proteins associated with MCV LT, we performed

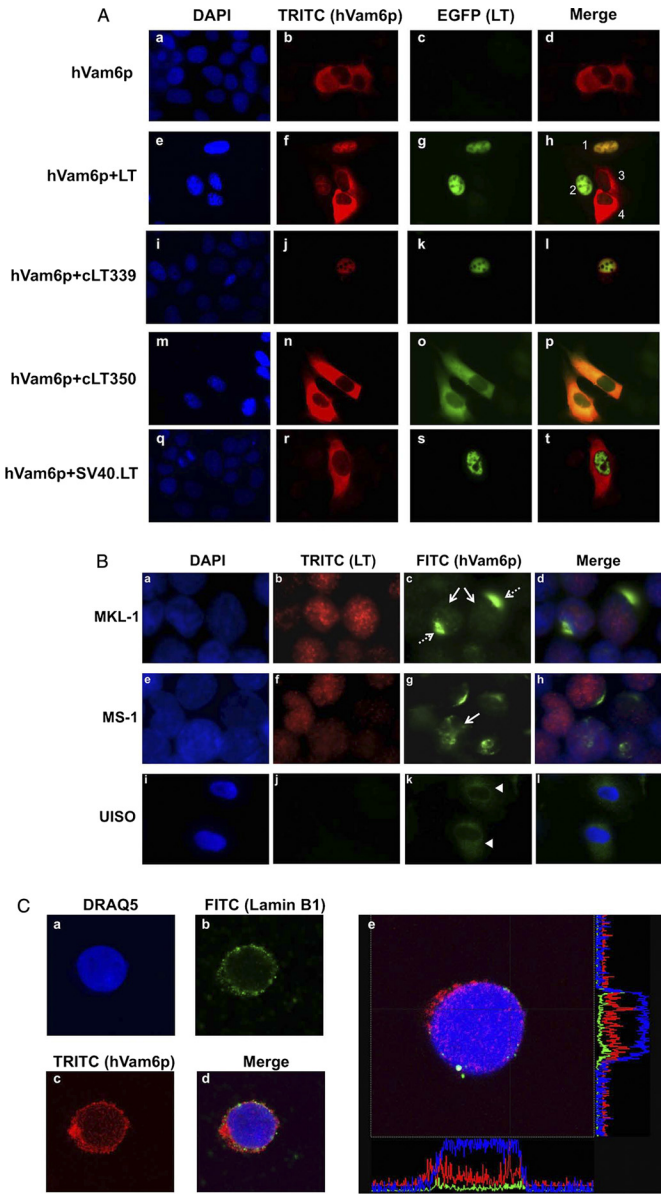

FIGURE 2. **Localization of hVam6p.** *A,* nuclear relocalization of hVam6p in U2OS cells during MCV LT expression. U2OS cells were transfected with Myc-hVam6p alone (*a–d*) or together with EGFP-LT (*e–h*), EGFP-cLT339 (*i–l*), EGFP-cLT350 (*m–p*), and EGFP-SV40.LT (*q–t*). The expression of hVam6p is visualized with anti-Myc antibody and Alexa Fluor 568-conjugated anti-mouse (TRITC), whereas the LTs are visualized by tagged EGFP fluorescence. hVam6p is present in the cytoplasm (*d*), but relocalized to the nucleus with wild-type LT expression (*h*). In a representative view of four cells (*1–4*), *1* and *2* contain both overexpressed wild type, full-length LT and hVam6p; whereas, cells *3* and *4* show only overexpressed hVam6p. hVam6p relocalizes to the nucleus only when LT is also present. Tumor-derived, truncated MCV LT protein (cLT339) also relocalize hVam6p (*l*), however, a tumor-derived MCV LT lacking a nuclear localization signal (cLT350) fails to relocalize hVam6p to the nucleus (*p*). No hVam6p relocalization is seen in conjunction with SV40 LT protein expression (*t*). *B,* immunofluorescence detection of endogenous hVam6p in naturally infected, MCV positive MKL-1 (*a–d*) and MS-1 (*e–h*) cell lines. Two patterns are seen. A portion of endogenous hVam6p shows an intranuclear localization similar to MCV LT (*solid arrow*), another portion demonstrates prominent perinuclear localization (*dashed arrow*) distinct from LT. In MCV negative UISO cell lines (*i–l*), no LT is expressed and hVam6p remains cytoplasmic (*arrowhead*). *C,* confocal microscopy of LT expressing MKL-1 cells shows hVamp6p (*c*) distributed largely in the same pattern as Lamin B1 (*b*), a marker for the nuclear membrane. In addition, hVam6p is also present in a diffuse pattern within the nuclear compartment (*c*). In *panel e* showing another typical cell, analyzed with cross-sectional graphing fluorescence intensity from DNA (*blue*), Lamin B1 (*green*), and hVamp6 (*red*) show increased hVam6p signal within the nuclear compartment defined by DNA and demarcated by Lamin B1.

TAP using two LT MUR fragments fused with N-terminal calmodulin-binding protein and streptavidin-binding protein tags (Fig. 1*A*). After stably expressing the dual-tag constructs in 293H cells, LT MUR interacting proteins were separated on SDS-PAGE gel. EGFP and SV40 T1–136 expressing controls were used to identify unique proteins only present in MCV LT samples. Following silver staining, a specific band at 120 kDa (Fig. 1*B*) was isolated and identified by mass spectrometry as hVam6p (hVps39). Rb was also recovered from this fraction, consistent with our previous report (2).

To confirm LT-hVam6p interaction, we performed a co-immunoprecipitation assay using U2OS cells overexpressing HA-hVam6p together with V5-tagged genomic LT (also expressing small T and 57 KT proteins), cDNA LT (cLT, expressing LT alone), or two tumor-derived LT (cLT339 and cLT350) proteins (Fig. 1*C*). All forms of MCV LT co-immunoprecipitated hVam6p, whereas no specific immunoprecipitation was found with the empty vector. To investigate endogenous interaction between hVam6p and MCV LT, the LT protein was immunoprecipitated using anti-MCV LT antibody CM2B4 (22). MCC cell lines harboring MCV (MKL-1, MS-1, and WaGa) were compared with MCV negative cell lines (UISO, MCC13, and MCC26). Immunoprecipitated proteins were immunoblotted with anti-hVam6p antibody (Fig. 1*D*). Robust immunoprecipitation was detected in MKL-1 and WaGa, and to a lesser extent in MS-1 cells but not in MCV-negative cell lines. These results indicate that hVam6p is an authentic binding partner for LT *in vivo*. Interaction between hVam6p, a cytoplasmic protein, and MCV LT, a nuclear protein is unexpected.

Co-localization of MCV LT and hVam6p—To determine that the interaction occurs in cells, we performed immunofluorescence localization of MCV LT and hVam6p. LT-EGFP fusion proteins and Myc-hVam6p were transiently overexpressed in U2OS cells followed by anti-Myc immunostaining. Immunofluorescence reveals that in the absence of MCV LT, hVam6p is distributed in the cytoplasm (Fig. 2*A*, *a–d*) as previously noted (15, 24). However, in the presence of MCV LT or cLT339, which both harbor nuclear localization signals, hVam6p translocates to the nucleus and co-localizes with LT (Fig. 2*A*, *e–h* and *i–l*). The naturally occurring tumor MCV cLT350 lacking an nuclear localization signals, however, co-localizes with hVam6p in the cytoplasm (Fig. 2*A*, *m–p*). SV40 LT does not co-localize or mislocalize hVam6p to the nucleus (Fig. 2*A*, *q–t*), consistent with hVam6p being an interactor specific for the MCV LT. We also examined endogenous hVam6p localization in MCV-positive MCC cell lines (MKL-1 and MS-1). Immunofluorescence shows that a portion of hVam6p is present in the nucleus (Fig. 2*B*, *c* and *g, solid arrow*). Additionally, in naturally infected MCV T antigen expressing Merkel cell carcinoma-derived cell lines, hVam6p also displays a perinuclear dot-like localization in a subpopulation of tumor cells (Fig. 2*B*, *c*, *dashed arrow*). In comparison, hVam6p is not relocalized to the nucleus in an MCV negative cell line, UISO (Fig. 2*B*, *i–l*). To confirm this, we performed confocal microscopy, which showed similar results as conventional fluorescence microscopy. hVam6p is present in the nucleus, colocalizes with Lamin B1 to the nuclear membrane, and focally in a perinuclear pattern. Analysis of single cell fluorescence profiles along two-dimensional axis shows intranuclear, nuclear membrane, as well as a perinuclear concentration of signal for hVam6p (Fig. 2*C*).

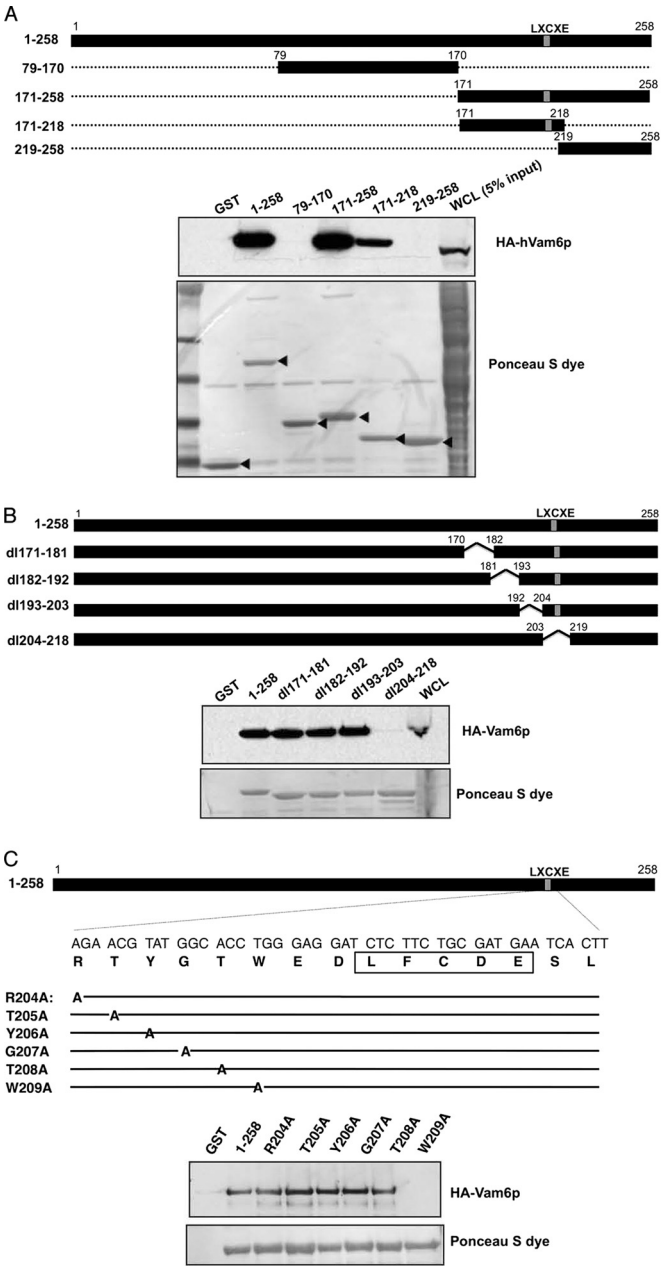

FIGURE 3. **Mapping the hVam6p binding site on MCV LT antigen.** *A*, diagram of GST-tagged LT deletion constructs. GST-LT fusion proteins were incubated with protein extracts of 293FT cells transfected with HA-hVam6p. Bound proteins were revealed by immunoblotting with anti-HA antibody (*top panel*). The GST fusion LT proteins were visualized by Ponceau S staining (*bottom panel*). *B*, further deletion analysis of the 171–218 subregion in the context of 1–258 LT. Ponceau S shows comparable expression of LT constructs and 1–258 has appropriately retarded migration (*bottom panel*). Co-immunoprecipitation shows that only dl204–218 loses the ability to interact with hVam6p (*top panel*). *C*, schematic diagram of MCV LT alanine substitution mutants based on localization of hVam6p binding to residues 204–218 (*A* and *B*). *LFCDE*, Rb-binding domain.

Fine Mapping of the MCV LT Domain Interacting with hVam6p—To better characterize the association of MCV LT and hVam6p, we mapped the domain of MCV LT necessary for its association with hVam6p. Using a series of LT MUR deletion

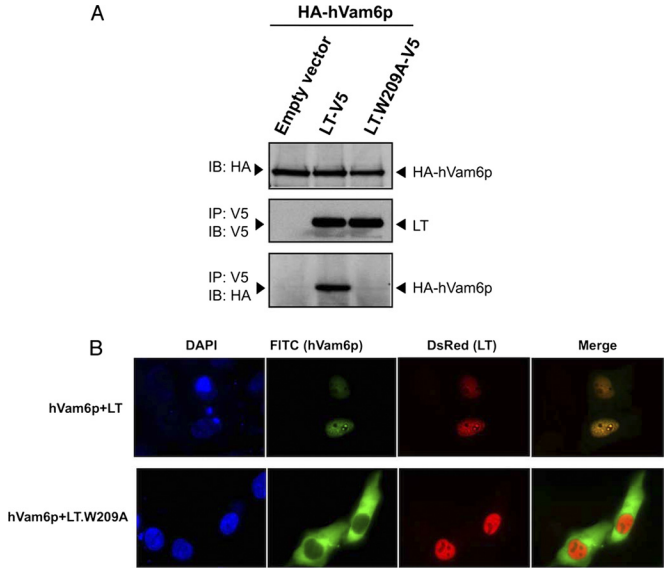

FIGURE 4. **MCV LT.W209A mutant is defective in interacting with and relocalizing hVam6p.** *A,* mutation at Trp-209 on full-length LT completely abolished LT-hVam6p binding. Lysates from U2OS cells transiently co-expressing HA-hVam6p with empty vector, LT-V5, or LT.W209A-V5 were immunoprecipitated (*IP*) for LT with anti-V5 antibody and immunoblotted (*IB*) for hVam6p by anti-HA antibody. *B,* LT.W209A fails to relocalize hVam6p to the nucleus. U2OS cells were co-transfected with Myc-hVam6p and LT-DsRed or LT.W209A-DsRed. hVam6p is visualized with anti-Myc antibody and Alexa Fluor 488-conjugated anti-mouse antibody (FITC), whereas the wild-type and mutant LTs are visualized by DsRed fluorescence.

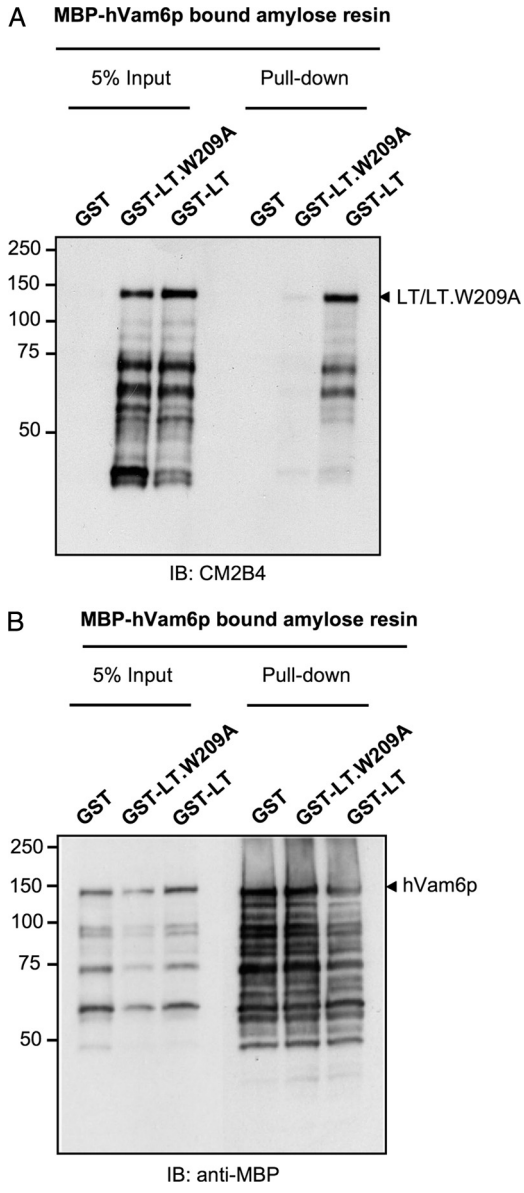

FIGURE 5. **Direct binding of MCV LT to hVam6p.** MBP-hVam6p-bound amylose resin beads were incubated with eluted GST, GST-LT.W209A, or GST-LT proteins for a pull-down assay. 5% input and bound proteins were separated on an 8% SDS-PAGE gel. Immunoblotting (*IB*) was performed with anti-MCV LT CM2B4 antibody (*A*) and anti-MBP antibody (*B*).

mutants (1–258, 79–170, 171–258, 171–218, and 219–258) fused to GST (Fig. 3*A*), we performed GST pulldowns on extracts from 293FT cells overexpressing hVam6p and found 171–218 to be the minimal fragment that binds hVam6p (Fig. 3*A*). Further mapping was performed using LT deletions created from this minimal region (dl171–181, dl182–192, dl193–203, and dl204–218); only the dl204–218 mutant was found to be defective in binding hVam6p (Fig. 3*B*). Six adjacent amino acid alanine substitution mutations (R204A, T205A, Y206A, G207A, T208A, and W209A) were then generated in the dl204–218 region (Fig. 3*C*, *top panel*). Trp-209 is positioned 2 residues N-terminal to the L*X*C*X*E domain and was found to be essential for hVam6p binding (Fig. 3*C*, *bottom panel*). This was confirmed by engineering the W209A substitution into full-length V5-tagged LT and performing immunoprecipitation in U2OS cells with HA-tagged hVam6p (Fig. 4*A*). The alanine substitution at LT Trp-209 completely abolishes LT interaction with hVam6p. When this alanine substitution is cloned into an EGFP-tagged LT (LT.W209A-EGFP), co-localization and nuclear translocation of hVam6p are lost (Fig. 4*B*).

To test if LT-hVam6p association is direct, we produced maltose-binding protein-tagged hVam6p (MBP-hVam6p), GST-LT, and GST-LT.W209A in bacteria, followed by a MBP pull-down assay. As shown in Fig. 5*A*, MBP-hVam6p specifically pulled down GST-LT, but not GST alone or the GST-LT.W209A mutant, indicating a direct binding of MCV LT to hVam6p. As shown in the *input* lanes, similar amounts of wild-type MCV LT and the mutant were used. Reprobing of the blot with MBP antibody revealed equivalent loading of MBP-hVam6p for all of the pull-downs (Fig. 5*B*).

Because Trp-209 is adjacent to the L*X*C*X*E Rb-binding motif, we tested whether a previously described mutation in the Rb binding motif (2) also affects hVam6p interaction with MCV LT. As seen in Fig. 6, substitution of lysine for glutamate at position 216 (LT.L*X*C*X*K), disrupts Rb interactions with LT (Fig. 6*A*) but has no effect on the hVam6p interaction with LT (Fig. 6*B*). Additionally, we tested the LT-hVam6p binding defective mutant LT.W209A and found it retains interaction with Rb (Fig. 6*C*). These findings suggest that Rb and hVam6p interaction domains are discrete sites. Because these two interaction sites are in close proximity, we next sought to determine whether hVam6p associates with Rb in the absence or presence of LT. As seen in Fig. 6*D*, hVam6p neither interacts with Rb directly, nor is bridged by LT to Rb. Similar results are found for the Rb family members, p107 and p130 (data not shown).

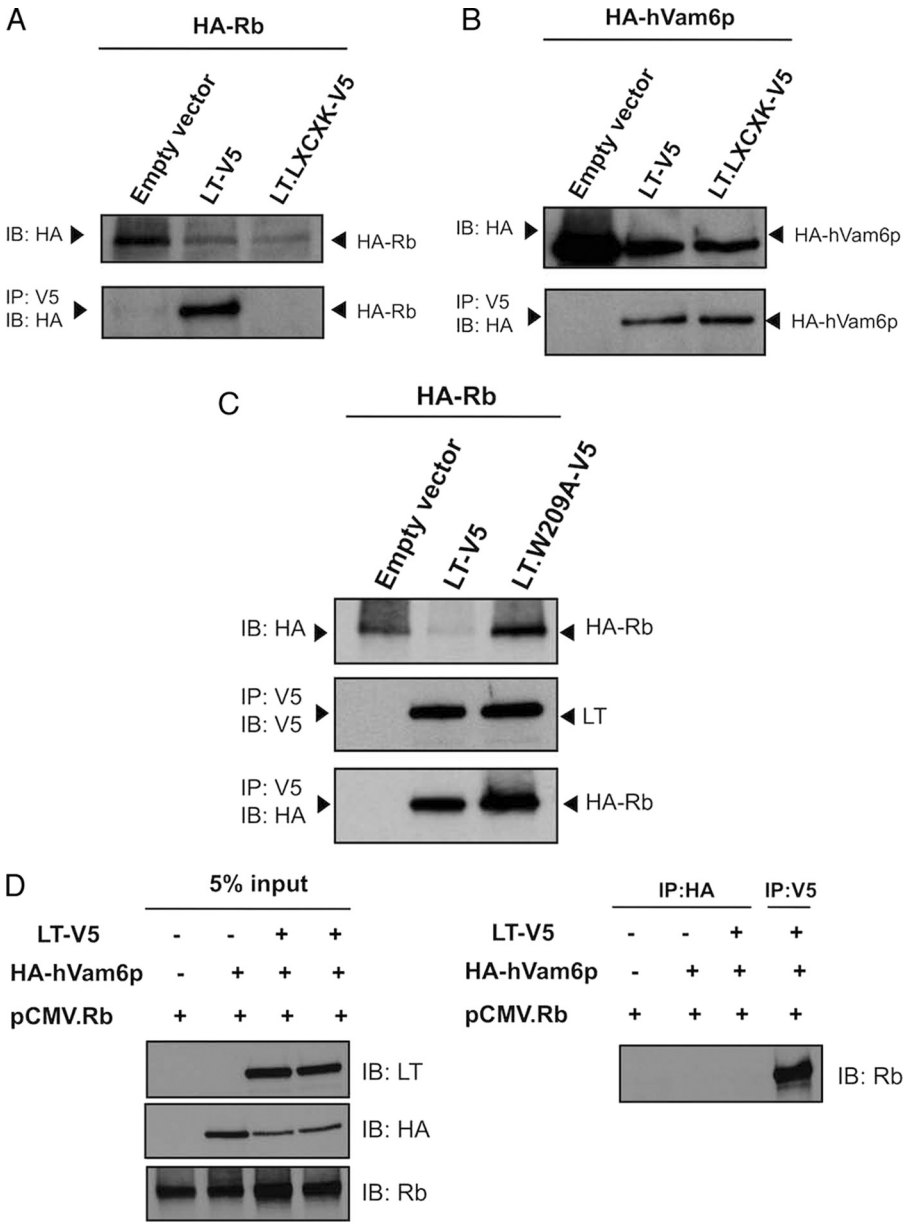

FIGURE 6. **Rb and hVam6p interaction domains are discrete sites on LT.** *A,* the LT.L*XCX*K mutant fails to bind Rb. U2OS cell lysates co-expressing HA-Rb with empty vector, LT, or Rb-binding mutant LT.L*XCX*K were immunoprecipitated for LT by anti-V5 antibody and immunoblotted for HA-Rb. *B,* LT.L*XCX*K mutant retains hVam6p interaction. U2OS cell lysates co-expressing HA-hVam6p with empty vector, LT, or Rb-binding mutant LT.L*XCX*K were immunoprecipitated for LT by anti-V5 antibody and immunoblotted for HA-hVam6p. *C,* LT.W209A mutant has no effect on Rb binding. U2OS cell lysates co-transfected with empty vector, LT, or LT.W209A were immunoprecipitated for LT by anti-V5 antibody and immunoblotted for HA-Rb. *D,* hVam6p does not associate with Rb in the presence or absence of LT. *Left panel,* 5% lysate input for LT, hVam6p, and Rb. *Right panel,* immunoprecipitation (*IP*) and immunoblotting (*IB*) for Rb.

Vam6p CLH Repeat Domain Is Responsible for Binding to MCV LT—hVam6p has a NH_2-terminal CNH domain and a central CLH repeat domain, both of which are required for lysosome clustering and fusion (15). We used a series of EGFP-tagged murine Vps39 (mVps39/mVam6p is near identical to hVps39/hVam6p) deletions (20) to map the LT binding site on mVps39 (Fig. 7*A*). U2OS cells were transfected with LT and mVps39 deletion mutants, followed by LT immunoprecipitation and immunoblotting for EGFP-mVps39. As seen in Fig. 7*B*, full-length mVps39 and mVps39 having the centrally located CLH domain and either N-terminal or C-terminal deletions all strongly interact with LT. In contrast, constructs lacking the CLH domain (CNH and Δ(CNH+CLH)) fail to interact with LT suggesting that the Vam6p CLH domain is critical in binding LT.

Functional Interactions of MCV LT with hVam6p: Lack of Effect on TGF-β and mTOR Signaling—Because hVam6p has been reported to be identical with the TRAP-1-like protein except for an 11-amino acid insertion and TRAP-1-like protein functions to balance Smad2 and Smad3 signaling (17), we examined the MCV LT effect on TGF-β signaling in HT1080 cells using the TGF-β-responsive luciferase reporter 3TP-Lux. Without TGF-β treatment, hVam6p expression has a minimal effect on basal 3TP-Lux activity but reporter activity nearly

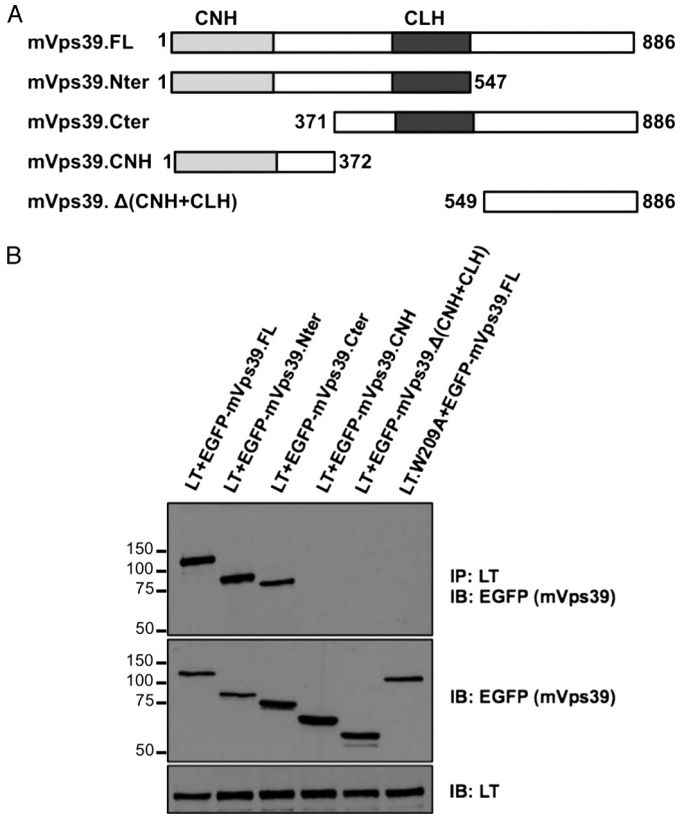

FIGURE 7. **Mapping of the LT binding site on Vam6p to regions containing the central clathrin homology repeat domain.** *A,* schematic representation of murine Vps39 (*mVps39*) and various deletion constructs. *B,* immunoprecipitation (*IP*) in U2OS cells of mVps39 deletions with MCV LT, using LT mutant as negative control (*last lane*). *Top panel,* immunoprecipitation (*IP*) of LT with CM2B4 antibody and immunoblotting (*IB*) of mVps39 with anti-EGFP antibody. *Middle panel,* 5% lysate input of each deletion construct. *Bottom panel,* 5% lysate input of LT or LT mutant.

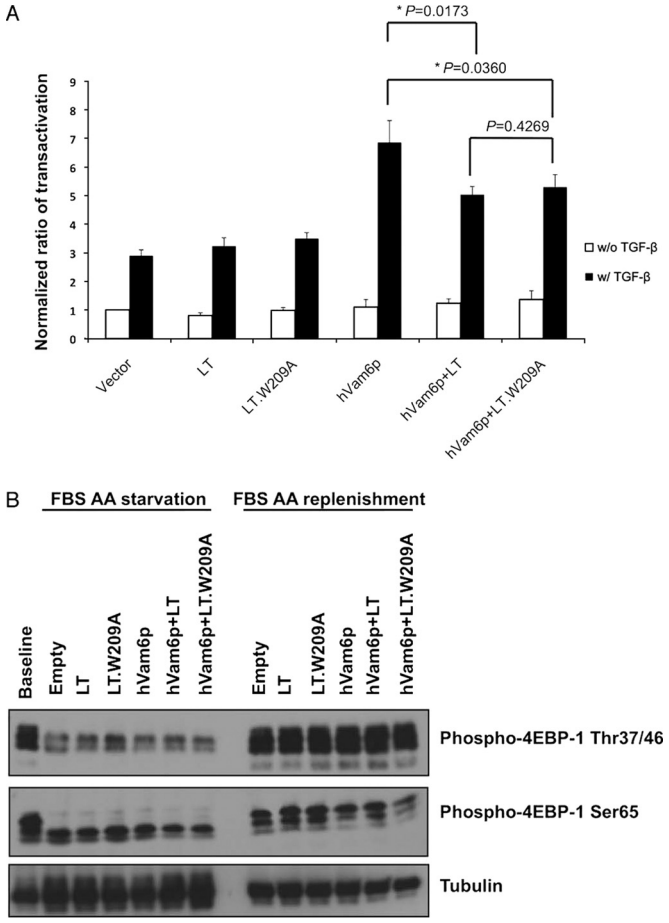

FIGURE 8. **Lack of effect on TGF-β and mTOR signaling.** *A,* LT-hVam6p binding has no significant effect on the TGF-β pathway. HT1080 cells were transfected with TGF-β inducible reporter p3TP-Lux and empty vector, wild-type LT, hVam6p binding mutant LT, alone or together with hVam6p. 24 h after transfection, cells were replaced with fresh DMEM with 0.2% FBS, left non-treated or stimulated with recombinant human TGF-β1 at 5 ng/ml for 18 h. Reporter activities were measured using the Dual Luciferase Reporter Assay System (Promega) and normalized to non-treated empty vector-transfected conditions. Independent experiments were performed in triplicate three times. *Error bars* and *p* values are shown. *B,* LT-hVam6p binding has no effect on the mTOR pathway. 293 cells were transfected with empty vector, wild-type LT, hVam6p binding LT mutant, alone or together with hVam6p, left in serum starvation (0.3% FBS) overnight. On the second day cells were starved in amino acid-free medium for 2 h and replenished with amino acid solution for 1 h. Non-stimulated and stimulated lysates were subjected to a Western blot analysis to probe for mTOR downstream of the target 4EBP-1 phosphorylation.

doubles with hVam6p expression after TGF-β treatment (Fig. 8*A*). LT expression modestly reduces this activity but this effect is independent of the LT.W209A substitution, suggesting that LT does not directly target TGF-β signaling through hVam6p (Fig. 8*A*).

Vam6p (Vps39 in yeast) also functions as a Rag family GTPase nucleotide exchange factor to promote TORC1 activation in response to increased amino acid concentrations in the environment of yeast, leading to mTOR-dependent phosphorylation of the cap-binding protein 4EBP-1 (26). To assess the effect of LT on mTOR signaling, we transfected 293 cells with HA-hVam6p together with wild-type LT or LT.W209A, alone or together with hVam6p. After overnight serum starvation and 2 h amino acid starvation, 4EBP-1 phosphorylation was assessed by Western blotting. Phospho-4EBP-1 Thr-37/46 and Ser-65 levels are low under starvation conditions compared with cells grown with serum and amino acids (baseline, Fig. 8*B*). hVam6p had no obvious activity on 4EBP-1 phosphorylation either during starvation or under replenished conditions. Furthermore, no significant or consistent change in 4EBP-1 phosphorylation was noted after expression of either the wild-type LT or LT.W209A (Fig. 8*B*).

MCV LT Disrupts hVam6p-induced Lysosome Clustering—A third function described for hVam6p overexpression is promotion of lysosome clustering (15, 24). HeLa cells were transiently transfected with LT or the hVam6p binding mutant, alone or together with Myc-hVam6p, and lysosome clustering was assessed by cytoplasmic clustering of lysosomal-associated membrane protein 1 (LAMP1). In the absence of hVam6p overexpression, there is no obvious difference between an empty vector, LT, and the mutant on LAMP1 staining (data not shown). Under standard growth conditions, LAMP1 shows a diffusely punctate distribution in the cytoplasm (Fig. 9, *a–d*). Overexpression of hVam6p induces perinuclear lysosome clustering as previously reported (15, 24) (Fig. 9, *e–h*). This clustering is abolished by expression of wild-type LT (Fig. 9, *i–l*) but not LT.W209A (Fig. 9, *m–p*). To determine whether nuclear sequestration of hVam6p is required for inhibition of lysosomal clustering, hVam6p was co-expressed with MCV350 LT, which lacks a nuclear localization signal but still interacts with

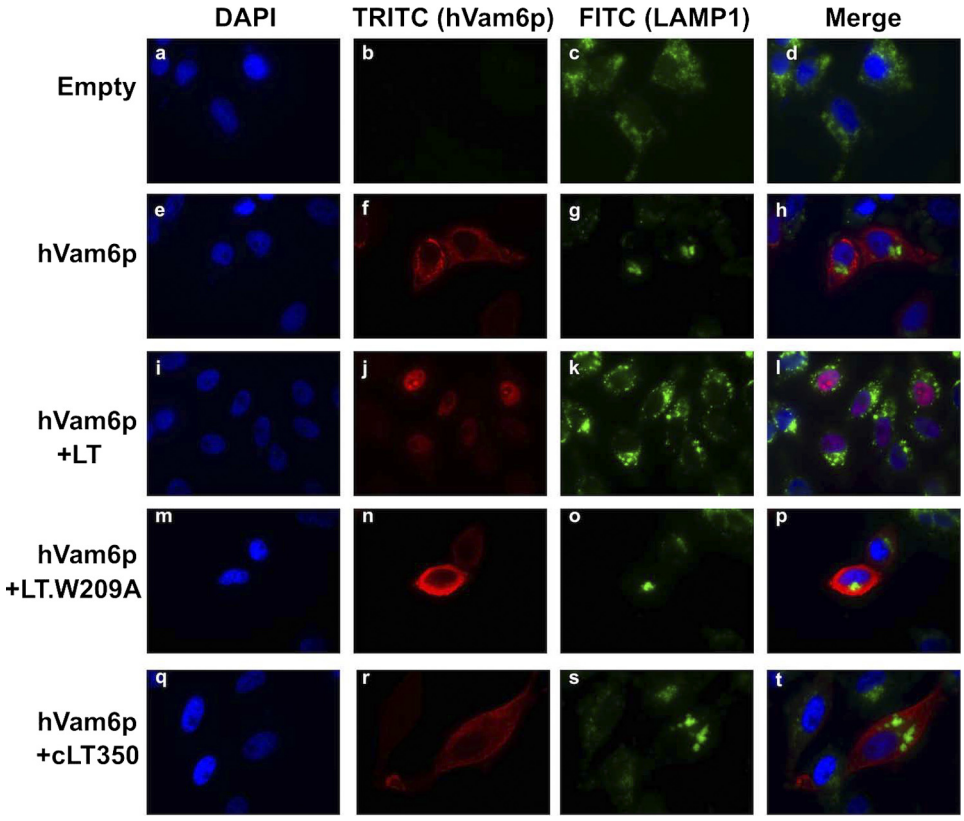

FIGURE 9. **LT inhibits hVam6p-induced lysosome clustering in HeLa cells.** HeLa cells were transfected with Myc-hVam6p alone (*e–h*), together with LT (*i–l*), LT.W209A (*m–p*), or cLT350 (*q–t*). The expression of hVam6p was visualized with anti-Myc antibody and Alexa Fluor 568-conjugated anti-mouse antibody (TRITC). LAMP1 was visualized with anti-human CD107a (LAMP1) Alexa Fluor 488. hVam6p-induced clustering of lysosomes (*h*) is lost when full-length LT (*l*) but not LT.W209A (*p*) or cLT350 (*t*) is co-expressed.

hVam6p (Fig. 2). Clustering was present with MCV350 LT expression (Fig. 9, *q–t*) suggesting that LT binding alone to hVam6p is insufficient to antagonize hVam6p-induced lysosomal clustering and nuclear sequestration is required to antagonize this effect.

DISCUSSION

We identified cytoplasmic human Vam6p as a unique interactor for nuclear MCV LT. The hVam6p interaction domain is not present in SV40 LT and we find that direct targeting of hVam6p does not occur with SV40 LT. To our knowledge, hVam6p has not been reported as a binding partner for any other viral protein. MCV LT associates with endogenous hVam6p in MCV positive cell lines making it likely that this interaction has physiological consequences. Interestingly, LT relocalizes hVam6p from the cytoplasm to the nucleus. Nuclear sequestration of a cytoplasmic protein is an unusual regulatory phenomenon that has been described for cytomegalovirus TRS-1 protein sequestration of protein kinase R (27), poliovirus-induced nuclear relocalization of eIF4E through eIF4G cleavage (28), and HPV-induced nuclear relocalization of p80 by the E1 protein (29). Although the MCV T antigen causes a loss-of-function for hVam6p involvement in lysosomal trafficking, we do not know if there is a subsequent gain-of-function via nuclear relocalization of hVam6p.

Current evidence indicates that MCV is a *bona fide* human cancer virus causing most cases of Merkel cell carcinoma (21). Like other human polyomaviruses, MCV is a common if not ubiquitous infection that does not normally integrate into the host chromosome as part of its life cycle. Virus mutation leads to genomic integration that contributes to tumor formation (1, 2). Integrated MCV genomes are clonal within tumors and most tumor cells express abundant LT protein (22). Expression of the full-length LT protein in cells harboring an integrated MCV genome, however, will lead to unlicensed replication from the integrated viral origin that is predicted to cause DNA fragmentation (2). Thus, additional virus mutations truncating the LT to eliminate its DNA replication capacity are commonly found in tumor-derived viruses. MCV species found in tumors are replication defective and do not represent free-living and transmissible viruses.

Our studies suggest the possibility that hVam6p sequestration might play a role in MCV replication rather than tumorigenesis. Unlike most MCV LT proteins, the tumor-derived MCV350 strain LT protein possesses a truncation that eliminates its nuclear localization signal (30). Most MCV LTs are localized to the nucleus, whereas MCV350 LT has a diffuse nuclear and cytoplasmic distribution. Although MCV350 LT still interacts with hVam6p, it does not inhibit lysosomal clustering. This circumstantial evidence suggests that this hVam6p antagonism by MCV LT involves nuclear sequestration rather than simple binding, and that this sequestration may not be critical to MCV-induced tumorigenesis. In a limited survey of TGF-β and mTOR signaling functions, we did not observe an effect for LT dependent on hVam6p interaction. We cannot

rule out the possibility that more extensive studies might reveal contributions to cell growth and proliferation by MCV LT targeting of hVam6p. In fact, interference with hVam6p function was found to enhance growth factor independent cell survival and potentially modulate autophagy (24, 31).

At present, there is no MCV replication system available to test for specific functions of LT in virus assembly, transmission, and replication but we anticipate that these questions can eventually be addressed using MCV molecular clone viruses. Because MCV is only found in high copy number in tumors, naturally occurring replication-competent MCV genomes have not been cloned until recently (32, 33).

Clues to the functions for MCV LT binding to hVam6p may come from infection studies of other polyomaviruses. Polyomaviruses make use of endosomal and lysosomal trafficking to transit from the cell membrane to the nucleus, although precise mechanisms differ between polyomaviruses (34). Murine polyomavirus, for example, binds the ganglioside GD1a and is transported to endolysosomes where pH-dependent conformational changes allow transport of the virus into the endoplasmic reticulum and then the nucleus for uncoating and replication (35). SV40 transit to the endoplasmic reticulum is dependent on viral coat protein binding initially to caveosomes and subsequently to caveolin-free membrane structures (36). Little is known about the cellular functions of hVam6p in lysosomal trafficking and many of its functions are inferred from studies of the yeast homolog, Vps39 (37). Disruption of Vps39 interaction with the C-Vps complex mislocalizes Vps39 from membrane-enriched subcellular fractions to the cytosolic fraction and causes hydrolase missorting defects, suggesting that localization of Vps39 to the vacuole is essential for vacuolar protein transport (38). Nuclear sequestration of hVam6p can be expected to affect its regulatory interactions with the C-Vps complex in human cells but it is unlikely to completely disrupt this complex. A class C-Vps component, hVps11, is not mislocalized by MCV LT protein expression (data not shown). Because LT is an early viral protein, it is more likely that targeting of hVam6p plays an important role in viral egress rather than entry.

Although we cannot completely exclude that some of the Piper hVam6p antibody reactivity could be nonspecific, every other alternative antibody tested, whether commercial (Proteintech, catalog number 16219-1-AP; rabbit polyclonal, Santa Cruz Biotechnology D-15; S14 goat polyclonals, Abcam mouse polyclonal ab69669, and rabbit polyclonal ab90516) or our own monoclonals, failed to react with endogenous hVam6p in immunoblots, although these antibodies often recognize the overexpressed protein. However, it is reassuring to us that the Piper antibody recognizes endogenous hVam6p coprecipitated with MCV LT in MCCs and it detects coprecipitated, overexpressed hVam6p, which interacts with wild-type MCV LT, but not the Trp-209 binding mutant. This coprecipitation pattern closely mirrors what we observe with HA-tagged hVam6p using HA antibody. Finally, the immunofluorescence pattern of nuclear and perinuclear staining observed in MCCs using the Piper antibody clearly overlaps with what we observe in heterologous cell systems using the tagged hVam6p. Future experiments, involving development of an independent antibody recognizing endogenous hVam6p, will establish the significance of the perinuclear localization in MCCs.

Our studies provide the first evidence for cytoplasmic targeting of endolysosomal components by a polyomavirus using a novel nuclear sequestration mechanism. MCV LT provides a unique reagent to study Vam6/Vps39 functions in cytoplasmic lysosomal trafficking. Development of robust MCV replication systems will allow examination of the consequences of hVam6p sequestration by LT to MCV infection.

Acknowledgments—We thank Dr. Robert C. Piper (University of Iowa) for hVam6p antibody; Dr. Juan S. Bonifacino (National Institutes of Health) for providing hVam6p expression plasmids; and Dr. J. Paul Luzio (University of Cambridge) for mVps39 deletion constructs. We thank Dr. Huichen Feng and Dr. Masa Shuda for generating pNTAP and LT-EGFP plasmids, and John Scofield for help with the manuscript. We are grateful to the Mass Spectrometry Core Facility (Beth Israel Deaconess Medical Center) for mass spectral analyses.

REFERENCES

1. Feng, H., Shuda, M., Chang, Y., and Moore, P. S. (2008) *Science* **319,** 1096–1100
2. Shuda, M., Feng, H., Kwun, H. J., Rosen, S. T., Gjoerup, O., Moore, P. S., and Chang, Y. (2008) *Proc. Natl. Acad. Sci. U.S.A.* **105,** 16272–16277
3. DeCaprio, J. A., Ludlow, J. W., Figge, J., Shew, J. Y., Huang, C. M., Lee, W. H., Marsilio, E., Paucha, E., and Livingston, D. M. (1988) *Cell* **54,** 275–283
4. Campbell, K. S., Mullane, K. P., Aksoy, I. A., Stubdal, H., Zalvide, J., Pipas, J. M., Silver, P. A., Roberts, T. M., Schaffhausen, B. S., and DeCaprio, J. A. (1997) *Genes Dev.* **11,** 1098–1110
5. Srinivasan, A., McClellan, A. J., Vartikar, J., Marks, I., Cantalupo, P., Li, Y., Whyte, P., Rundell, K., Brodsky, J. L., and Pipas, J. M. (1997) *Mol. Cell. Biol.* **17,** 4761–4773
6. Lane, D. P., and Crawford, L. V. (1979) *Nature* **278,** 261–263
7. Linzer, D. I., and Levine, A. J. (1979) *Cell* **17,** 43–52
8. Cotsiki, M., Lock, R. L., Cheng, Y., Williams, G. L., Zhao, J., Perera, D., Freire, R., Entwistle, A., Golemis, E. A., Roberts, T. M., Jat, P. S., and Gjoerup, O. V. (2004) *Proc. Natl. Acad. Sci. U.S.A.* **101,** 947–952
9. Ali, S. H., Kasper, J. S., Arai, T., and DeCaprio, J. A. (2004) *J. Virol.* **78,** 2749–2757
10. Pallas, D. C., Shahrik, L. K., Martin, B. L., Jaspers, S., Miller, T. B., Brautigan, D. L., and Roberts, T. M. (1990) *Cell* **60,** 167–176
11. Whitman, M., Kaplan, D. R., Schaffhausen, B., Cantley, L., and Roberts, T. M. (1985) *Nature* **315,** 239–242
12. Campbell, K. S., Ogris, E., Burke, B., Su, W., Auger, K. R., Druker, B. J., Schaffhausen, B. S., Roberts, T. M., and Pallas, D. C. (1994) *Proc. Natl. Acad. Sci. U.S.A.* **91,** 6344–6348
13. Dilworth, S. M., Brewster, C. E., Jones, M. D., Lanfrancone, L., Pelicci, G., and Pelicci, P. G. (1994) *Nature* **367,** 87–90
14. Pipas, J. M. (1992) *J. Virol.* **66,** 3979–3985
15. Caplan, S., Hartnell, L. M., Aguilar, R. C., Naslavsky, N., and Bonifacino, J. S. (2001) *J. Cell Biol.* **154,** 109–122
16. Price, A., Seals, D., Wickner, W., and Ungermann, C. (2000) *J. Cell Biol.* **148,** 1231–1238
17. Felici, A., Wurthner, J. U., Parks, W. T., Giam, L. R., Reiss, M., Karpova, T. S., McNally, J. G., and Roberts, A. B. (2003) *EMBO J.* **22,** 4465–4477
18. Li, L., and Guan, K. L. (2009) *Mol. Cell* **35,** 543–545
19. Flinn, R. J., Yan, Y., Goswami, S., Parker, P. J., and Backer, J. M. (2010) *Mol. Biol. Cell* **21,** 833–841
20. Poupon, V., Stewart, A., Gray, S. R., Piper, R. C., and Luzio, J. P. (2003) *Mol. Biol. Cell* **14,** 4015–4027
21. Houben, R., Shuda, M., Weinkam, R., Schrama, D., Feng, H., Chang, Y., Moore, P. S., and Becker, J. C. (2010) *J. Virol.* **84,** 7064–7072
22. Shuda, M., Arora, R., Kwun, H. J., Feng, H., Sarid, R., Fernández-Figueras,

M. T., Tolstov, Y., Gjoerup, O., Mansukhani, M. M., Swerdlow, S. H., Chaudhary, P. M., Kirkwood, J. M., Nalesnik, M. A., Kant, J. A., Weiss, L. M., Moore, P. S., and Chang, Y. (2009) *Int. J. Cancer* **125,** 1243–1249
23. Richardson, S. C., Winistorfer, S. C., Poupon, V., Luzio, J. P., and Piper, R. C. (2004) *Mol. Biol. Cell* **15,** 1197–1210
24. Peralta, E. R., Martin, B. C., and Edinger, A. L. (2010) *J. Biol. Chem.* **285,** 16814–16821
25. Wrana, J. L., Attisano, L., Cárcamo, J., Zentella, A., Doody, J., Laiho, M., Wang, X. F., and Massagué, J. (1992) *Cell* **71,** 1003–1014
26. Binda, M., Péli-Gulli, M. P., Bonfils, G., Panchaud, N., Urban, J., Sturgill, T. W., Loewith, R., and De Virgilio, C. (2009) *Mol. Cell* **35,** 563–573
27. Hakki, M., Marshall, E. E., De Niro, K. L., and Geballe, A. P. (2006) *J. Virol.* **80,** 11817–11826
28. Sukarieh, R., Sonenberg, N., and Pelletier, J. (2010) *J. Gen. Virol.* **91,** 1224–1228
29. Côté-Martin, A., Moody, C., Fradet-Turcotte, A., D'Abramo, C. M., Lehoux, M., Joubert, S., Poirier, G. G., Coulombe, B., Laimins, L. A., and Archambault, J. (2008) *J. Virol.* **82,** 1271–1283
30. Nakamura, T., Sato, Y., Watanabe, D., Ito, H., Shimonohara, N., Tsuji, T., Nakajima, N., Suzuki, Y., Matsuo, K., Nakagawa, H., Sata, T., and Katano, H. (2010) *Virology* **398,** 273–279
31. Liang, C., Lee, J. S., Inn, K. S., Gack, M. U., Li, Q., Roberts, E. A., Vergne, I., Deretic, V., Feng, P., Akazawa, C., and Jung, J. U. (2008) *Nat. Cell. Biol.* **10,** 776–787
32. Schowalter, R. M., Pastrana, D. V., Pumphrey, K. A., Moyer, A. L., and Buck, C. B. (2010) *Cell Host Microbe* **7,** 509–515
33. Laude, H. C., Jonchere, B., Maubec, E., Carlotti, A., Marinho, E., Couturaud, B., Peter, M., Sastre-Garau, X., Avril, M. F., Dupin, N., and Rozenberg, F. (2010) *PLoS Pathog.* **6,** e1001076
34. Mannová, P., and Forstová, J. (2003) *J. Virol.* **77,** 1672–1681
35. Qian, M., Cai, D., Verhey, K. J., and Tsai, B. (2009) *PLoS Pathog.* **5,** e1000465
36. Pelkmans, L., Fava, E., Grabner, H., Hannus, M., Habermann, B., Krausz, E., and Zerial, M. (2005) *Nature* **436,** 78–86
37. Nakamura, N., Hirata, A., Ohsumi, Y., and Wada, Y. (1997) *J. Biol. Chem.* **272,** 11344–11349
38. Wurmser, A. E., Sato, T. K., and Emr, S. D. (2000) *J. Cell Biol.* **151,** 551–562